A&A 613, A46 (2018)
https://doi.org/10.1051/0004-6361/201731982

Astronomy & Astrophysics

Asteroseismology of ZZ Ceti stars with full evolutionary white dwarf models

II. The impact of AGB thermal pulses on the asteroseismic inferences of ZZ Ceti stars

F. C. De Gerónimo[1,2], L. G. Althaus[1,2], A. H. Córsico[1,2], A. D. Romero[3], and S. O. Kepler[3]

[1] Grupo de Evolución Estelar y Pulsaciones, Facultad de Ciencias Astronómicas y Geofísicas, Universidad Nacional de La Plata, Paseo del Bosque s/n, 1900 La Plata, Argentina
e-mail: fdegeronimo@fcaglp.unlp.edu.ar
[2] Instituto de Astrofísica de La Plata (IALP - CONICET) Paseo del Bosque s/n, 1900 La Plata, Buenos Aires, Argentina
[3] Departamento de Astronomia, Universidade Federal do Rio Grande do Sul, Av. Bento Goncalves 9500, Porto Alegre 91501-970, RS, Brazil

Received 22 September 2017 / Accepted 30 January 2018

ABSTRACT

Context. The thermally pulsing phase on the asymptotic giant branch (TP-AGB) is the last nuclear burning phase experienced by most low- and intermediate-mass stars. During this phase, the outer chemical stratification above the C/O core of the emerging white dwarf (WD) is built up. The chemical structure resulting from progenitor evolution strongly impacts the whole pulsation spectrum exhibited by ZZ Ceti stars, which are pulsating C/O core white dwarfs located on a narrow instability strip at $T_{\rm eff} \sim 12\,000$ K. Several physical processes occurring during progenitor evolution strongly affect the chemical structure of these stars; those found during the TP-AGB phase are the most relevant for the pulsational properties of ZZ Ceti stars.
Aims. We present a study of the impact of the chemical structure built up during the TP-AGB evolution on the stellar parameters inferred from asteroseismological fits of ZZ Ceti stars.
Methods. Our analysis is based on a set of carbon–oxygen core white dwarf models with masses from 0.534 to 0.6463 $M_{\odot}$ derived from full evolutionary computations from the ZAMS to the ZZ Ceti domain. We computed evolutionary sequences that experience different number of thermal pulses (TP).
Results. We find that the occurrence or not of thermal pulses during AGB evolution implies an average deviation in the asteroseimological effective temperature of ZZ Ceti stars of at most 8% and on the order of $\lesssim$5% in the stellar mass. For the mass of the hydrogen envelope, however, we find deviations up to 2 orders of magnitude in the case of cool ZZ Ceti stars. Hot and intermediate temperature ZZ Ceti stars show no differences in the hydrogen envelope mass in most cases.
Conclusions. Our results show that, in general, the impact of the occurrence or not of thermal pulses in the progenitor stars is not negligible and must be taken into account in asteroseismological studies of ZZ Ceti stars.

Key words. asteroseismology – stars: oscillations – white dwarfs – stars: evolution – stars: interiors

1. Introduction

After the end of core He burning, single low- and intermediate-mass stars of up to 8–10 $M_{\odot}$ experience the last nuclear burning phase in their evolution while ascending along the asymptotic giant branch (AGB); this phase is known as thermal pulses (TP). Stars at this evolutionary stage are composed by a C/O core, which is a product of the core He-burning stage, that is surrounded by a He burning shell, and surrounded itself by a He buffer and an outer H-burning shell. As the star begins to ascend to the AGB, the H-burning layer is turned off. After its reignition, the He shell becomes unstable and the star begins the thermally pulsing stage (TP-AGB).

The interplay between mixing and burning that occurs along the TP-AGB leaves marked imprints on the chemical stratification of the outer layers of the emerging white dwarf (WD), see Althaus et al. (2010a). Indeed, during the TP-AGB, third dredge-up episodes yield appreciable surface composition changes, as a result of which the star becomes C enriched. In addition, some stars may experience hot bottom burning (HBB) episodes in which the bottom of the convective envelope penetrates into the top of the H-burning shell producing N, Na, and Al (Karakas & Lattanzio 2014). Most importantly for the inner chemical stratification that characterizes the emerging WD is the formation of an intershell region rich in He and C during the TP-AGB phase that is left by the short-lived He flash induced convection zone at the peak flash. The mass of this intershell (and the position of the core–He transition) depends strongly on both the occurrence of overshooting (OV) during the He flash and the number of TP. The latter is determined by the initial mass, composition, and the poorly constrained efficiency of the mass loss rate (Karakas & Lattanzio 2014). It should be mentioned that, despite the relevance of the occurrence of TPs for the chemical structure of the outer layers of WDs, their consequences for the asteroseismological fits of ZZ Ceti stars are not usually taken into account and have not been assessed. Although the TP-AGB phase is expected for most WD progenitors, it is possible that some WDs could have resulted from progenitor

stars that avoided this phase. For instance, it is well known that low-mass He-burning stars located at the extreme horizontal branch, and thus characterized by extremely thin H envelopes, are expected to evolve directly to the WD stage, thereby avoiding the AGB, the so-called AGB-Manqué and post early AGB stars (Greggio & Renzini 1990). In line with this, recent evidence suggests that most He-rich stars of NGC2808 do not reach the AGB phase, evolving directly to the WD state after the end of the He core burning (Marino et al. 2017). In addition, departure from the AGB before reaching the TP-AGB phase as a result of mass transfer by binary interaction (Pustynski & Pustylnik 2006; Han et al. 2000) or envelope ejection by the swallowing of a planet or a very low-mass companion (De Marco & Soker 2002) is also possible.

In view of these considerations, we must consider that a fraction of WDs have evolved from progenitors that avoided the TP-AGB phase. This being the case, differences in the chemical structure of the outermost layers of the C/O core should be expected according to whether the progenitor stars evolved through the TP-AGB or not, with consequences for the expected pulsational properties of pulsating WDs.

In the context of the preceeding discussion, it is well known that the precise shape of the chemical abundance distribution in H-rich (DA) WDs is critical for the pulsational properties of variable DA WDs (ZZ Ceti stars). ZZ Ceti (or DAV) variable stars are located in an instability strip with effective temperatures between 10 500 and 12 500 K (Fontaine & Brassard 2008; Winget & Kepler 2008; Althaus et al. 2010b; Kepler & Romero 2017), and constitute the most numerous class of compact pulsators. These stars are characterized by multimode photometric variations caused by non-radial g-mode pulsations of low harmonic degree ($\ell \leq 2$) with periods between 70 and 1500 s and amplitudes up to 0.30 mag. These pulsations are thought to be excited by both the κ–γ mechanisms acting on the base of the H partial ionization zone (Dolez & Vauclair 1981; Winget et al. 1982) and the "convective driving" mechanism (Brickhill 1991; Goldreich & Wu 1999; Saio 2013). Since the discovery of the first ZZ Ceti star, HL Tau 76 by Landolt (1968), a continuous effort has been made to model the interior of these variable stars.

From the asteroseismological analysis of DAVs, i.e., the comparison of the observed periods in variable DA WDs with those computed from theoretical models, details about the previous evolutionary history of the star can be inferred. This analysis allows us to constrain several stellar parameters such as the stellar mass, thickness of the outer envelopes, core chemical composition, and stellar rotation rates (e.g., Romero et al. 2012). In addition, ZZ Ceti asteroseismology is a valuable tool for studying axions (Isern et al. 1992, 2010; Bischoff-Kim et al. 2008; Córsico et al. 2012, 2016) and crystallization (Montgomery et al. 1999; Córsico et al. 2004, 2005; Metcalfe et al. 2004; Kanaan et al. 2005; Romero et al. 2013).

Two main approaches have been adopted for WD asteroseismology. The first employs static stellar models with parametrized chemical profiles. This approach has the advantage that it allows a full exploration of the parameter space to find an optimal seismic model (Bradley 1998, 2001; Castanheira & Kepler 2009; Bischoff-Kim & Østensen 2011; Bischoff-Kim et al. 2014), ultimately leading to good matches to the periods (Giammichele et al. 2017a,b). As precise as they have become, parameterized approaches rely on an educated guess of the internal composition profiles, owing the large number of parameters involved and the small number of periods typically available. Such profiles come from fully evolutionary models, which is the approach we follow in this work. The models are generated by tracking the complete evolution of the progenitor star, from the zero age main sequence (ZAMS) to the WD stage (Romero et al. 2012, 2013). This approach involves the most detailed and updated input physics, in particular regarding the internal chemical structure expected from the nuclear burning history of the progenitor, which is a crucial component of correctly disentangling the information encoded in the pulsation patterns of variable WDs. This asteroseismic approach allows us not only to unveil the interior structures of stars, but also find out how a star gets to that structure. This method has been successfully applied in various classes of pulsating WDs (see Romero et al. 2012, 2013; Córsico & Althaus 2006; Córsico et al. 2006, 2009, in the case of ZZ Ceti, DB, and PG1159 stars, respectively).

However, none of these asteroseismological approaches take into account the current uncertainties in stellar evolution, neither in the modeling nor in the input physics of WD progenitors. In this regard, De Gerónimo et al. (2017) explored for the first time the impact of the occurrence of TP in WD progenitors, the uncertainty in the $^{12}C(\alpha,\gamma)^{16}O$ cross section, and the occurrence of extra mixing on the expected period spectrum of ZZ Ceti stars. These authors reported that the chemical profiles built up during the TP-AGB phase impact markedly the g-mode pulsational periods, and concluded that the occurrence or not of the TP-AGB phase constitutes a relevant issue that has to be taken into account in seismological fits of these stars.

In view of the findings by De Gerónimo et al. (2017), the present paper is focused on assessing the role played by the TP-AGB phase of progenitor stars in the stellar parameters inferred from asteroseismological fits to artificial and real ZZ Ceti stars. To do this we first computed evolutionary sequences from the ZAMS to the TP-AGB stage. During the AGB, we forced the models to leave this stage at two instances: previous to the first thermal pulse and at the end of the third thermal pulse, thus generating two sets of evolutionary models. Next, we followed the evolution of the progenitors to the WD state until the domain of the ZZ Ceti instability strip, where we computed the period spectrum. Finally, we performed the asteroseismological analysis to sets of random periods representative of ZZ Ceti stars and later to real stars by considering the two sets of models.

This work is part of an ongoing project in which we will assess uncertainties in evolutionary history of WD progenitors and their impact on the pulsational properties and asteroseismological fits to ZZ Ceti stars. The work is organized as follows: in Sect. 2 we introduce the numerical tools employed and the input physics assumed in the evolutionary calculations together with the pulsation code employed. In Sect. 3 we present our results and, finally, in Sect. 4 we conclude the paper by summarizing our findings.

2. Computational tools

2.1. Evolutionary code and input physics

The DA WD evolutionary models computed in this work were generated with the LPCODE evolutionary code. The LPCODE produces detailed WD models in a consistent way with the predictions of progenitor history. The code is based on an updated physical description (Althaus et al. 2005, 2010a; Renedo et al. 2010; Romero et al. 2012; Miller Bertolami 2016) and was employed to study various aspects of the evolution of low-mass stars (Wachlin et al. 2011; Althaus et al. 2013, 2015), formation of horizontal branch stars (Miller Bertolami et al. 2008), extremely low-mass WDs (Althaus et al. 2013), AGB, and post-AGB evolution (Miller Bertolami 2016). We enumerate below

the most important physical parameters relevant to this work as follows: (i) for pre-WD stages, we adopted the standard mixing-length theory with the free parameter $\alpha = 1.61$. (ii) Diffusive OV during the evolutionary stages prior to the TP-AGB phase was allowed to occur following the description of Herwig et al. (1997). We adopted $f = 0.016$ for all sequences. The occurrence of OV is relevant for the final chemical stratification of the WD (Prada Moroni & Straniero 2002; Straniero et al. 2003). (iii) Breathing pulses, which occur at the end of core He burning, were suppressed (see Straniero et al. 2003, for a discussion on this topic). (iv) A simultaneous treatment of non-instantaneous mixing and burning of elements were considered. Our nuclear network accounts explicitly for the following 16 elements: ^{1}H, ^{2}H, ^{3}He, ^{4}He, ^{7}Li, ^{7}Be, ^{12}C, ^{13}C, ^{14}N, ^{15}N, ^{16}O, ^{17}O, ^{18}O, ^{19}F, ^{20}Ne, and ^{22}Ne, and 34 thermonuclear reaction rates (Althaus et al. 2005). (v) Gravitational settling and thermal and chemical diffusion were taken into account during the WD stage for ^{1}H, ^{3}He, ^{4}He, ^{12}C, ^{13}C, ^{14}N, and ^{16}O (Althaus et al. 2003). (vi) During the WD phase, chemical rehomogenization of the inner C–O profile induced by Rayleigh–Taylor (RT) instabilities was implemented following Salaris et al. (1997). (vii) For the high-density regime characteristic of WDs, we used the equation of state of Segretain et al. (1994), which accounts for all the important contributions for both the liquid and solid phases.

Our evolutionary sequences were computed considering all the evolutionary stages of the WD progenitor, including the stable core He burning and the TP-AGB and post-AGB phases. It is worth mentioning that LPCODE has been compared against other WD evolution code, showing 2% differences in the WD cooling times that come from the different numerical implementations of the stellar evolution equations (Salaris et al. 2013).

2.2. Pulsation code

We employed the LP-PUL adiabatic non-radial pulsation code described in Córsico & Althaus (2006) for the pulsation analysis presented in this work. The LP-PUL code is coupled to the LPCODE evolutionary code and solves the full fourth-order set of real equations and boundary conditions governing linear, adiabatic, and non-radial stellar pulsations. The LP-PUL code provides the eigenfrequency $\omega_{\ell,k}$, where k is the radial order of the mode, and the dimensionless eigenfunctions $y_1, \ldots, y_4$. The LP-PUL code computes the periods ($\Pi_{\ell,k}$), rotation splitting coefficients ($C_{\ell,k}$), oscillation kinetic energy ($K_{\ell,k}$), and weight functions ($W_{\ell,k}$). The expressions to compute these quantities can be found in the Appendix of Córsico & Althaus (2006). The Brunt-Väisälä frequency (N) is computed as (Tassoul et al. 1990)

$$N^2 = \frac{g^2\rho}{p}\frac{\chi_{\rm T}}{\chi_\rho}(\nabla_{\rm ad} - \nabla + B), \tag{1}$$

where

$$B = -\frac{1}{\chi_{\rm T}}\sum_{i=1}^{n-1}\chi_{X_{\rm i}}\frac{{\rm d}\ln X_{\rm i}}{{\rm d}\ln\rho} \tag{2}$$

is the Ledoux term and contains the contribution coming from the chemical composition changes, and

$$\chi_{\rm T} = \left[\frac{\partial\ln p}{\partial\ln T}\right]_\rho \quad \chi_\rho = \left[\frac{\partial\ln p}{\partial\ln\rho}\right]_{\rm T} \quad \chi_{X_i} = \left[\frac{\partial\ln p}{\partial\ln X_i}\right]_{\rho,T,X_{j\neq i}}. \tag{3}$$

In what follows we describe how we generated the synthetic random-period spectra by means of a uniform distribution function. Even though the observed periods of real ZZ Ceti stars do not come from a uniform distribution and in fact DAV stars actually show a set pattern, this is not an issue because we use a quality function that self-selects the representative periods of ZZ Ceti stars. This is further detailed in Sect. 2.3. Particularly, with our method, we quickly generated a huge number of synthetic period spectra. These spectra were used to perform a statistical approach to assess the impact of the uncertainties coming from the TP phase on the asteroseismologically derived stellar parameters. Finally this approach allows us to carry out full exploration of the impact on the stellar parameters of ZZ Ceti models representative of stars from the blue and red edge of the instability strip separately.

2.3. Synthetic set of periods

In our first analysis we concentrated on asteroseismological fits performed to sets of random synthetic periods. We generated 1000 sets of three random periods (i.e., 1000 artificial pulsating stars), representative of ZZ Ceti stars, from the $RANDOM function in BASH. The $RANDOM returns a pseudo-random integer with a periodicity of $16 \times (2^{31}-1)$. Then, we performed asteroseismological fits to those artificial stars and compared the respective stellar parameters that were obtained.

As shown by Mukadam et al. (2006), those observed pulsating WDs located at the blue edge of the ZZ Ceti instability strip are characterized by pulsation modes with periods <350 s with small amplitudes, whilst those located at the red edge are characterized by pulsation modes with periods >650 s and larger amplitudes. Motivated by these findings, we performed the asteroseismological fits and the corresponding analyses for the following period ranges: $\Pi_i < 350$ s (RI), $350 < \Pi_i < 650$ s (RII), and $\Pi_i > 650$ s (RIII).

To find our best-fit model we searched for the model that best matches the pulsation periods of our artificial stars. To do this, we calculated a quality function as in Castanheira & Kepler (2008), and find for the model that minimizes it

$$\phi = \phi(M_\star, M_{\rm H}, T_{\rm eff}) = \frac{1}{N}\sqrt{\sum_{i=1}^{N}\frac{[\Pi_I{\rm th} - \Pi_i^{\rm obs}]^2 A_i}{\sum_{i=1}^{N} A_i}}, \tag{4}$$

where the amplitudes A_i are used as weights of each observed period. We used our artificial periods as if they were observed periods and fixed the amplitudes as $A_i = 1$. Since generally our quality function leads to very similar results as compared with those coming from a quality function that does not take into account the mode amplitude, we describe the quality of our period fits in terms of ϕ (Romero et al. 2012). We set a threshold value of the quality function, $\phi_{\rm lim}$, and disregarded those models characterized by $\phi > \phi_{\rm lim}$. For artificial stars with periods in RI, we set $\phi_{\rm lim} = 6$ s, while for artificial stars with periods in the ranges RII and RIII, we set $\phi_{\rm lim} = 3$ s. These limit values are motivated from a balance between the amount of possible seismical solutions that satisfies the condition $\phi < \phi_{\rm lim}$ and the smallest possible difference between the periods corresponding to the model and those characterizing the synthetic period spectra. Out of the complete set of models, we find only 153 best-fit models in the range RI, 293 in RII, and 620 in RIII.

At the outset, our synthetic periods were generated randomly with a uniform distribution. However, by virtue of the constraint $\phi < \phi_{\rm lim}$, the effective periods – those which correspond to a best-fit model – are clustered at around 100, 170, 270, and 340 s, as depicted in Fig. 1. This is in line with the findings of Clemens et al. (2017) that, in hot ZZ Ceti stars,

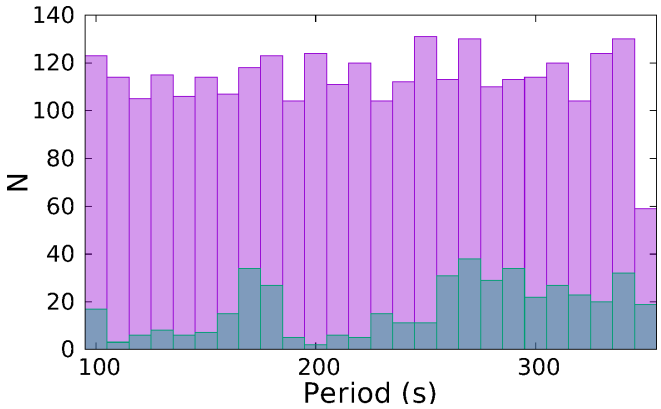

Fig. 1. Histograms of the 3000 random periods in RI (pink bars) and of those of the 153 artificial stars which satisfy $\phi < 6$ (effective periods: green bars).

the pulsation periods are arranged in groups separated by gaps. Specifically, by comparing the observational periods with those from theoretical evolutionary computations of Romero et al. (2012), Clemens et al. (2017) found that the existence of these gaps is in agreement with models with a thick hydrogen layer mass. In addition, Clemens et al. (2017) compared period groupings with those obtained by performing Monte Carlo simulations using the period grid from Romero et al. (2012) with different assumptions, and concluded that most of the hot ZZ Ceti have $M_{\rm H}$ values at or near the canonical limit with He layers thinner than those predicted by evolutionary models. As we see later, this result is in agreement with what we found. These period patterns are not found when studying the remaining ranges of periods RII and RIII.

3. Models and asteroseismological fits

In this section, we study the impact of the occurrence of TPs during the progenitor evolution on the parameters of ZZ Ceti stars derived by means of asteroseismology. As we mentioned, even though the occurrence of the TP-AGB phase is expected for most WD progenitors, there is diverse evidence that some WDs could have resulted from progenitor stars that avoided this phase. In this context, as shown in De Gerónimo et al. (2017), whether the progenitor star evolves through the TP-AGB or does not strongly impacts the period spectrum of pulsating DA WDs, especially in the case of the low-mass ZZ Ceti stars.

To this end, we developed a grid of evolutionary models with progenitor masses in the range $0.85 \leq M_{\rm ZAMS}/M_{\odot} \leq 2.25$ (final masses in the range $0.5349 \lesssim M_{\rm wd}/M_{\odot} \lesssim 0.6463$) from the ZAMS to the TP-AGB phase. On the AGB, we forced the evolutionary models to abandon this stage by enhancing the stellar mass loss rate at two different stages: previous to the onset of the first thermal pulse and at the end of the third thermal pulse (0TP and 3TP models, respectively). As a result of the pulse driven convection zone that develops at each TP, a double-layered chemical structure with an intershell region rich in C and He at the bottom of the He buffer is expected (Althaus et al. 2010a). The size of this intershell and the precise shape of the chemical profile characterizing the double-layered region depend on the number of TPs experienced by the progenitor as it evolves along the TP-AGB phase. In particular, as a consequence of the outward moving He-burning shell, the size of the intershell decreases and the core/He chemical transition shifts to outer layers. Nevertheless, it is during the first TP that the main chemical features of the intershell and the double-layered regions emerge. In the case of low-mass stars, we do not expect the occurrence of a large number of TP, so considering three TP is enough to capture the essence of the chemical structure arising from TP-AGB phase. For higher stellar masses, we expect a larger number of TPs to take place, but as shown in De Gerónimo et al. (2017), the period spectrum expected at the ZZ Ceti stage is not markedly affected by the number of additional TPs experienced by the progenitor star; see their Fig. 3 (a and b). Once the progenitor leaves the AGB phase, we continue its evolution to the WD cooling phase until the ZZ Ceti stage, where we calculated the period spectrum. In Fig. 2 we show the internal chemical profiles for the most abundant elements of our models (upper panel) and the logarithm of the squared Brunt-Väisälä (B-V) frequency (lower panel) in terms of the outer mass fraction for models with $M_{\rm ZAMS} = 1.00\,M_{\odot}$, at the ZZ Ceti stage ($T_{\rm eff} \sim 12\,000$ K). For the 3TP model, three chemical transition regions from center to the surface can be noticed: an inner chemical interface of C and O, an intermediate interface rich in He, C, and O that separates the core from the intershell region rich in He and C, and finally an interface separating the intershell region from the pure helium buffer. An additional interface separating the pure H and He envelopes, not shown in the figure, is also present in the outermost layers. The bumps in the B–V frequency induced by these transition regions, strongly affect the pulsation spectrum and mode trapping properties. The imprints of the occurrence of TPs on the B–V frequency result from both the shift in the position of the core/He transition and the presence of the intershell region that emerges during the TP-AGB phase. As shown in De Gerónimo et al. (2017), the intershell region survives down to the ZZ Ceti stage only for low-mass WD stars. This is because diffusion processes acting on the WD cooling phase are less efficient for the less massive stars. On the other hand, for more massive models, this intershell region is almost completely eroded by the action of element diffusion; see Fig. 1 (b) of De Gerónimo et al. (2017). We mention that in our seismological fits we have taken into account different values for the H content of the WD. In particular, we considered the H envelope mass to vary from the canonical value[1] to $\log(M_{\rm H}/M_{\rm wd}) \sim -9$.

To account for the differences induced in the stellar parameters of asteroseismological models of ZZ Ceti stars resulting from considering or not the TP-AGB phase, we performed period-to-period fits to a large number of artificial stars that were generated by considering several sets of three $\ell = 1$ mode periods. Based on the work of Mukadam et al. (2006), we explored the impact on artificial stars belonging to different period ranges. In order to find the best-fit solution, we considered the quality function ϕ [Eq. (4)], and search for its minimum – that is, the best period-fit model – in both 0TP and 3TP sets of models. In general, when asteroseismological fits are performed with real data, external determinations such as effective temperature, stellar mass, or surface gravity can be used as filters to discard models that are in disagreement with observational parameters (see Romero et al. 2012, Sect. 4.3.1). In the case of artificial stars, we were unable to use external constraints because the synthetic periods were generated randomly without any assumption at the outset. In this case, the results presented here reveal the differences between best-fit models according to the lowest value of the quality function only. In what follows, we compare the differences in the most relevant parameters of the asteroseismological

[1] The value predicted from fully evolutionary computations.

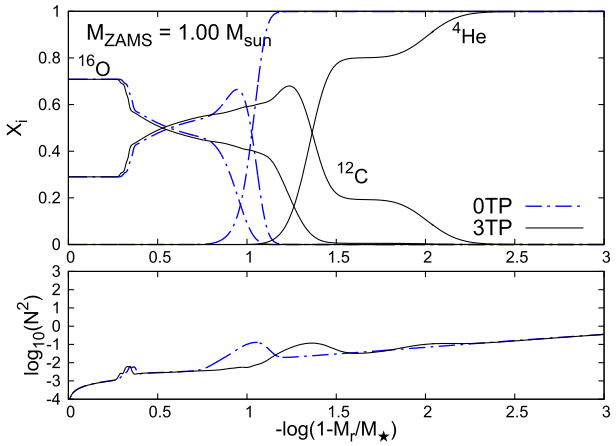

Fig. 2. Internal chemical abundances for the most abundant species of our 0TP and 3TP models for a 1 $M_{\odot}$ progenitor at the ZZ Ceti stage ($M_{\rm wd}$ = 0.5508 $M_{\odot}$). During the evolution through the first three TPs the core–He transition shifts from $-\log(q) \sim 1$ to ∼1.3 and the intershell region is built up.

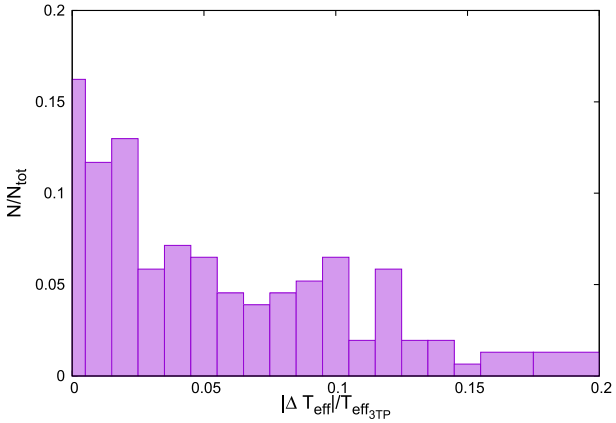

Fig. 3. Histogram for the absolute differences in effective temperature between our best fits for the 0TP and 3TP sets of models in the [95–350] s period range.

models when they are derived from the sets of 0TP and 3TP models.

3.1. Impact over stellar parameters

We employ a set of synthetic periods between 95 and 350 s (typical of hot ZZ Ceti stars), between 350 and 650 s (typical of ZZ Ceti stars in the middle of the instability strip), and between 650 and 1250 s (typical of cool ZZ Ceti stars). Periods with values $\Pi_i \in$ [95–350 s] are associated with low-radial order modes and usually they probe the inner structure of the star. However, some of these modes could be sensitive to the outer layers of the star.

In Figs. 3–7 we show histograms for the absolute difference in $T_{\rm eff}$, $M_{\rm wd}$ and $\log(M_{\rm H}/M_{\rm wd})$ between our 0TP and 3TP best-fit models. These histograms represent the percentage ($N/N_{\rm Tot}$, y-axis) of artificial models with a given amount of variation in the respective quantity[2] ($|\Delta T_{\rm eff}|/T_{\rm eff(3TP)}$, $|\Delta M_{\rm wd}|/M_{\rm wd(3TP)}$, $M_{\rm H}/M_{\rm wd}$, x-axis). In order to compare the deviations found in the values of $M_{\rm H}/M_{\rm wd}$, we plot the difference $|\log(M_{\rm H}/M_{\rm wd})_{\rm 0TP} - \log(M_{\rm H}/M_{\rm wd})_{\rm 3TP}|$.

[2] We take the models that experience three TP as our reference models.

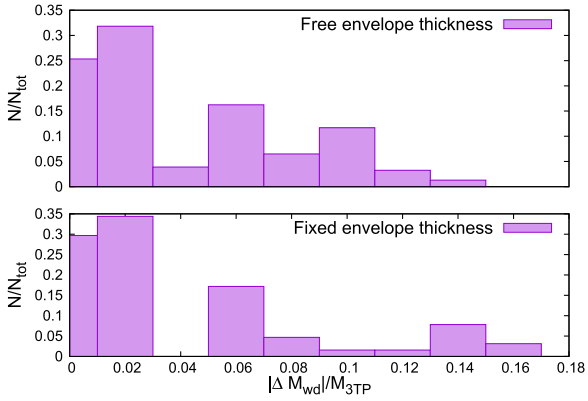

Fig. 4. Histogram of the differences for differences in the stellar mass.

From Fig. 3 we see that most of the relative differences in effective temperature between both sets of fits for hot ZZ Cetis are concentrated toward low values of $|\Delta T_{\rm eff}|$. A similar trend is also found for intermediate-$T_{\rm eff}$ and cool ZZ Ceti models. We fit a Gaussian function of the form $f(x) = A \cdot \exp(-(x - x_0)^2/(2 \cdot \sigma^2))$ to the histogram and obtain that the mean deviation in effective temperature is roughly 700 K. The mean deviation is ∼500 and ∼800 K for intermediate-$T_{\rm eff}$ and cool ZZ Ceti stars, respectively. Although these mean variations may exceed the expected observational uncertainties (Tremblay et al. 2011), it is worth noting that more than 50% of the fits show differences lower than ∼300 K.

Figure 4 shows the expectations for the differences in the stellar mass. In the upper panel, we show a histogram of the differences that result when we allow all the parameters to vary freely. This histogram displays several maxima at $|\Delta M_{\rm wd}|/M_{\rm wd(3TP)} \sim 0.005, 0.02, 0.06, 0.11$. For cool ZZ Ceti models, we find that the number of cases showing larger differences increases. The occurrence of several maxima is probably linked to the well-known core–envelope degeneracy related to the existence of a symmetry in the mode-trapping properties that can lead to an ambiguity in determining the location of features in the chemical structure (see Montgomery et al. 2003, for details). To break this possible degeneracy, we perform all the asteroseismological fits again, but this time by considering a fixed H envelope mass of $\sim 10^{-6} M_{\rm wd}$ for all the models. The results are depicted in the lower panel of Fig. 4. Even though some maximum still remains, about 70% of the cases now show differences smaller than the spectroscopic uncertainties, which can rise up to 4–5%[3]. We emphasize that these differences in the stellar mass of the best-fit models come from the fact that models with different stellar masses have different core chemical structure. For instance the extension in mass of the core and also the central chemical abundances of carbon and oxygen depend on the stellar mass (Althaus et al. 2010a; Romero et al. 2012).

The distribution of the differences in $M_{\rm H}/M_{\rm wd}$ resulting from the two sets of evolutionary sequences is shown in the histograms shown in Figs. 5–7. For the short period range, i.e., hot ZZ Ceti models (Fig. 5), most of the fits are clustered around $|\log(M_{\rm H}/M_{\rm wd})_{\rm 0TP} - \log(M_{\rm H}/M_{\rm wd})_{\rm 3TP}| \sim 0$, i.e., no differences in the H envelope mass are expected in most cases due to uncertainties in TP-AGB evolution. By contrast, as we consider cooler ZZ Ceti models, uncertainties in the TP-AGB phase

[3] When we fix the envelope mass, the effects on the distribution in $T_{\rm eff}$ are less pronounced. In particular, the peak at ∼0.1 (Fig. 3) is reduced and the number of the cases with deviations within 5% increases.

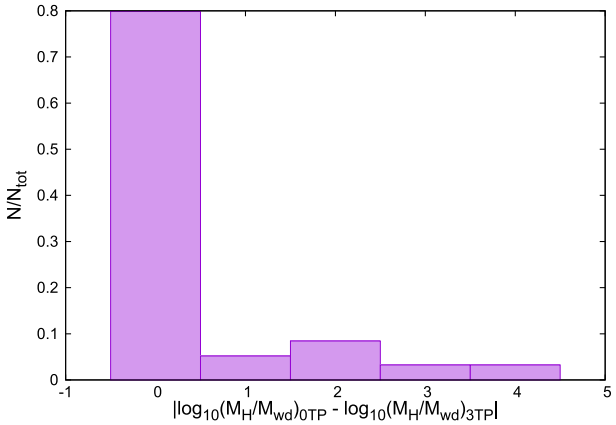

Fig. 5. Histogram for the differences in the determination of the H envelope mass for the period range [95–350] s.

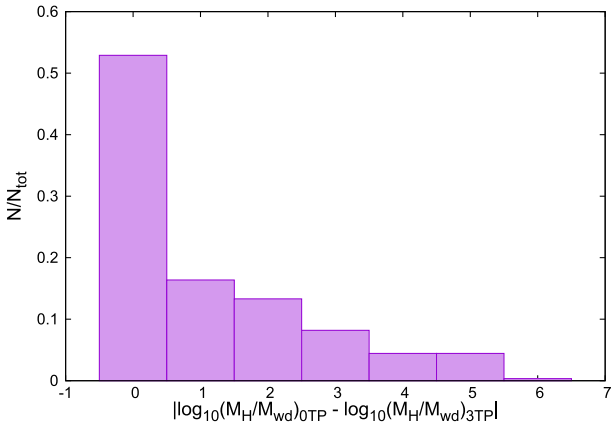

Fig. 6. Same as Fig. 5 but for fits considering the 350–650 s period range.

impact markedly the inferred H envelope mass (Figs. 6 and 7). This is not an unexpected behavior, since some of the pulsational modes of high radial order characterizing cool ZZ Ceti stars are sensitive to the outer chemical structure. A Gaussian fit to the data yields a mean deviation of $M_{\rm H}$ well below than an order of magnitude for hot and intermediate-$T_{\rm eff}$ models and 2 orders of magnitude for cool ZZ Ceti models. Clearly, for hot and intermediate ZZ Ceti models, the occurrence or not of TP during the AGB evolution of progenitor stars translates into uncertainties in the derived H envelope mass of less than one order of magnitude in most cases. This is not the trend for the case of cool ZZ Ceti models.

3.2. Asteroseismological fits to real ZZ Ceti

We contrast the results of the previous section with those derived from asteroseismological fits to some selected real ZZ Ceti stars. We picked out those ZZ Ceti stars with modes previously identified as $\ell = 1$ and whose spectroscopic masses fall into the mass range considered in this work. Spectroscopic determinations of $T_{\rm eff}$ and $M_{\rm wd}$ of the selected ZZ Ceti stars are shown in Table 1. We classified these stars as cool, intermediate-$T_{\rm eff}$, or hot ZZ Ceti stars depending on the value of the pulsation period with the highest amplitude. For the asteroseismological analysis and selection of the best-fit models, we took into account the following criteria described in Sect. 4.3.1 of Romero et al. (2012):

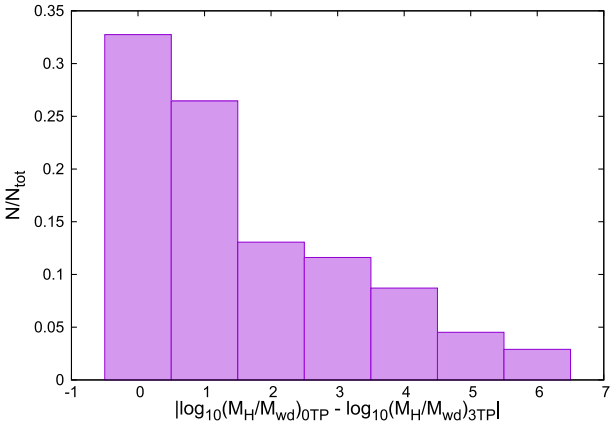

Fig. 7. Same as Fig. 5 but for fits considering the 650–1250 s period range.

Table 1. Spectroscopic determinations of $T_{\rm eff}$ and $M_{\rm wd}/M_{\odot}$ corresponding to the ZZ Ceti stars selected in this work.

Star	$T_{\rm eff}$	$M_{\rm wd}/M_{\odot}$	Reference
KUV 11370+4222	11 890	0.639	Bergeron et al. (2004)
HE 0031−5525	11 480	0.44	Castanheira et al. (2006)
WD J1002+5818	11 710	0.57	Mullally et al. (2005)
WD J0214−0823	11 570	0.57	Mukadam et al. (2004)
BPM 31594	11 450	0.666	Bergeron et al. (2004)
G191−16	11 420	0.632	Bergeron et al. (2004)
MCT 0145−2211	11 500	0.684	Bergeron et al. (2004)
WD J150−0001	11 200	0.61	Mukadam et al. (2004)
HE 1429−037	11 434	0.514	Silvotti et al. (2005)
EC 23487−2424	11 520	0.661	Bergeron et al. (2004)
G232−38	11 350	0.610	Gianninas et al. (2006)

– The models minimize the quality function given by Eq. (4), and therefore the observed periods are closely matched by the theoretical periods.
– We consider only those stars with assigned $\ell = 1$ modes in previous asteroseismological analysis.
– We elect those models with $T_{\rm eff}$ and $\log(g)$ as close as possible to the spectroscopic determinations.

The results of the asteroseismological period-to-period fits are illustrated in Fig. 8, which shows the deviations found in the derived stellar parameters as given by the two sets of evolutionary sequences. In this figure, we plot the percentage of the deviation in effective temperature and stellar mass, together with the absolute difference in $\log(M_{\rm H}/M_{\rm wd})$, as given by the color scale to the right. The differences in $T_{\rm eff}$ resulting from the occurrence of TPs range from 0.4% to 7.1%. The differences in stellar mass are in the range 0.9–6%, except for G191−16, for which the difference in stellar mass amounts to 17%. Although we might expect a certain link between the magnitude of the deviations found in the different stellar parameters, we did not find a clear pattern. Another important result from Fig. 8 is that, independent of the periods exhibited by the stars, a wide range of colors is seen, i.e., some hot- and even intermediate-effective temperature ZZ Ceti stars are sensitive to the thickness of the hydrogen envelope. There were some hints before that even low radial overtone modes could be sensitive to the structure in the outer layers of the models. For instance, Romero et al. (2012) found that a low k mode in the hot ZZ Ceti G117-B15A was very sensitive to the mass of the hydrogen envelope.

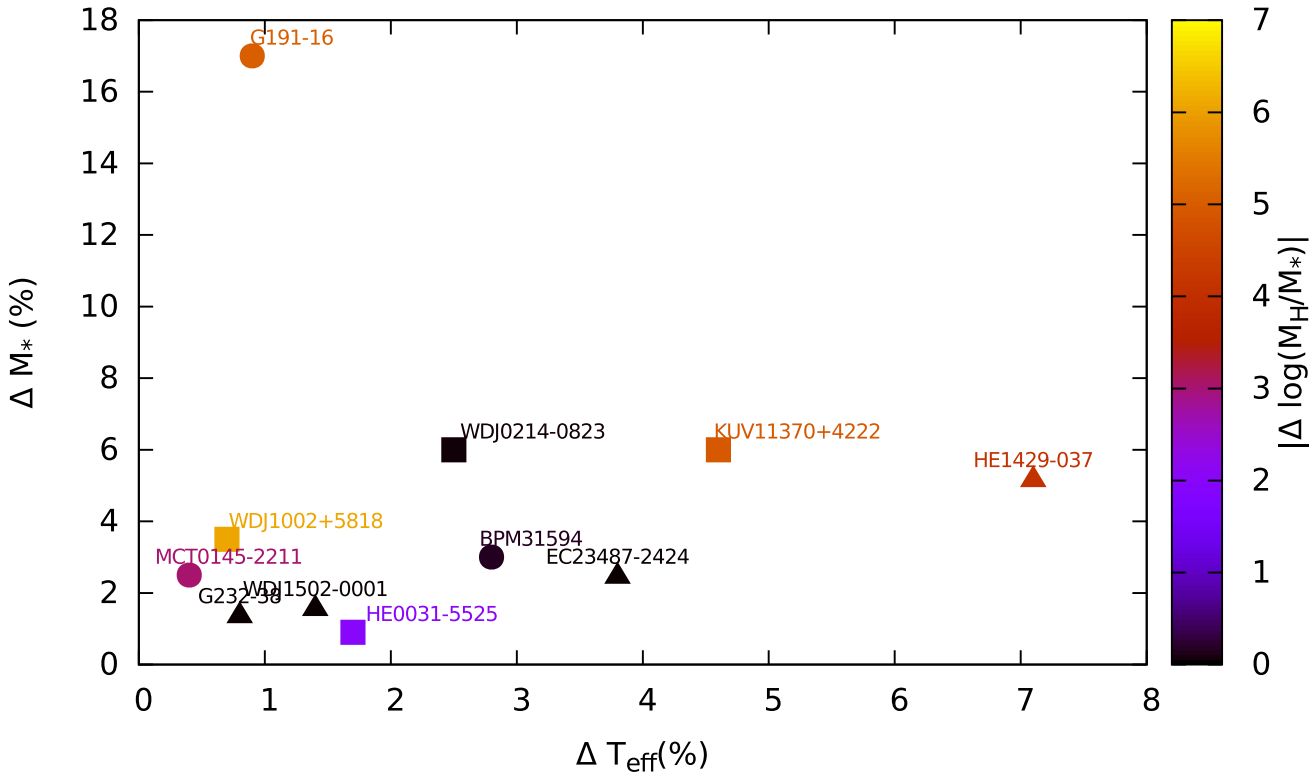

Fig. 8. Variations of $T_{\rm eff}$, $M_{\rm wd}$, and $M_{\rm H}$ – in color scale – of selected ZZ Ceti stars resulting from the two sets of evolutionary sequences considered in this work. Squares, circles, and triangles refer to hot, intermediate, and cool ZZ Ceti stars, respectively.

4. Summary and conclusions

In this work, we have studied the impact of the occurrence of TPs during the AGB evolution of the WD progenitor stars on the stellar parameters of ZZ Ceti stars as derived from asteroseismological period fits to artificial and real ZZ Ceti stars. To this end, we evolved progenitor star models with initial masses in the range 0.85–2.25 $M_{\odot}$ from the ZAMS to the TP-AGB phase. Here, we forced the progenitor to abandon the AGB at two stages: previous to the occurrence of the first TP and at the end of the third TP. In this way, we generated two sets of evolutionary sequences, 0TP and 3TP. All of the resulting sequences were evolved along the WD stage down to the domain of the ZZ Ceti stars, at $T_{\rm eff} \sim 12\,500$–$10\,500$ K. At this stage, we computed the theoretical period spectrum for each model. Asteroseismological period-to-period fits were carried out for a set of random periods as well as to the period spectra of selected real ZZ Ceti stars.

Marked differences in the pulsational period spectrum are expected depending on whether the progenitor star evolves through the TP-AGB phase or not. We find that this translates into a non-negligible impact for the resulting asteroseismological fits, depending on the period range exhibited by the star. We report that the fact that a WD progenitor experiences the TP-AGB phase or not implies an average deviation of the effective temperature of the asteroseismological models for ZZ Ceti stars of at most 8% (with more than 50% of the fits showing differences lower than 300 K) and on the order of $\lesssim 5\%$ in the stellar mass (with more than 70% of the fits showing differences lower than the spectroscopic uncertainties). For the mass of the H envelope, however, we find deviations up to 2 orders of magnitude in the case of cool ZZ Ceti models. For hot and intermediate ZZ Ceti models, no differences in the H envelope mass is expected in most cases from the occurrence of TP during AGB evolution. These trends remain when real ZZ Ceti stars are considered. We also find that the period spectrum of some hot and intermediate effective temperature ZZ Ceti stars are sensitive to the thickness of the hydrogen envelope (see Fig. 8).

This paper, which is part of an ongoing project, assesses for the first time the uncertainties in progenitor evolution – particularly the occurrence of the TP-AGB phase – and their impact on stellar parameters inferred from asteroseismological period fits to ZZ Ceti stars. Even though the TP-AGB phase is expected to be a common phase for most WD progenitors, evidence is mounting that some WDs could have been formed from progenitor stars that avoided this phase; for instance, this would be the case for most of the He rich stars in NGC2808, which fail to reach the AGB phase, thus evolving directly to the WD state after the end of the He core burning (Marino et al. 2017). As shown in De Gerónimo et al. (2017) the occurrence or not of TPs is the main uncertainty in progenitor evolution that mostly affects the expected pulsational periods of ZZ Ceti stars. As far as asteroseismology is concerned, the results found in this paper show that the imprints left by the occurrence of the TPs during AGB evolution of progenitor star are not negligible and must be taken into account in asteroseismological fits of these stars.

As stated before, two main asteroseismological avenues are currently being applied to peering into the interior of WDs, and both methods are complementary to each other. On the one hand, there is the approach that considers stellar models with parametrized chemical composition profiles. This is a powerful method that has the flexibility of allowing a full exploration of the parameter space to find an optimal asteroseismological model. The downside of this method is that sometimes it can lead to WD asteroseismological models with chemical structures that are not predicted by stellar evolution (e.g., the existence of a pure C buffer and unrealistic abundances of C and O at the core). The second approach, developed at La Plata Observatory, is different in nature, as it employs fully evolutionary models

that are the result of the complete evolution of the progenitor stars, from the ZAMS until the WD phase. This method involves the most detailed and updated input physics, in particular regarding the internal chemical structure expected from the nuclear burning history of the progenitor, a crucial aspect for correctly disentangling the information encoded in the pulsation patterns of variable DA WDs. However, we emphasize that this method is affected by several important uncertainties connected with evolutionary processes during the progenitor star evolution. A specific assessment of the impact of these uncertainties on the properties of asteroseismological models of ZZ Ceti stars derived with this method was lacking. This paper intends to fill this gap. Specifically, in this paper and in De Gerónimo et al. (2017) we have demonstrated that the uncertainties in prior WD evolution affect WD asteroseismology, but that the effects are quantifiable and bounded. Indeed, differences in stellar mass, effective temperature, and H envelope thickness due to the occurrence or not of TP at the AGB phase, the main uncertainty resulting from the evolutionary history of progenitor star, are within the typical spectroscopic errors. These results add confidence to the use of fully evolutionary models with consistent chemical profiles, and render our asteroseismological approach much more robust. In order to complete this critical evaluation of our asteroseismological method, we plan to present a future paper that addresses the impact of the uncertainties in the $^{12}C(\alpha,\gamma)^{16}O$ nuclear reaction rate on the asteroseismological inferences of ZZ Ceti stars (De Geronimo et al., in prep.).

Acknowledgements. We acknowledge the valuable comments of our referee that substantially improved the original version of this paper. We warmly acknowledge the helpful comments of J. J. Hermes. Part of this work was supported by AGENCIA through the Programa de Modernización Tecnológica BID 1728/OC-AR and by the PIP 112-200801-00940 grant from CONICET. This research has made use of NASA Astrophysics Data System.

References

Althaus, L. G., Serenelli, A. M., Córsico, A. H., & Montgomery, M. H. 2003, A&A, 404, 593
Althaus, L. G., Serenelli, A. M., Panei, J. A., et al. 2005, A&A, 435, 631
Althaus, L. G., Córsico, A. H., Bischoff-Kim, A., et al. 2010a, ApJ, 717, 897
Althaus, L. G., Córsico, A. H., Isern, J., & García-Berro, E. 2010b, A&ARv, 18, 471
Althaus, L. G., Miller Bertolami, M. M., & Córsico, A. H. 2013, A&A, 557, A19
Althaus, L. G., Camisassa, M. E., Miller Bertolami, M. M., Córsico, A. H., & García-Berro, E. 2015, A&A, 576, A9
Bergeron, P., Fontaine, G., Billères, M., Boudreault, S., & Green, E. M. 2004, ApJ, 600, 404
Bischoff-Kim, A., & Østensen, R. H. 2011, ApJ, 742, L16
Bischoff-Kim, A., Montgomery, M. H., & Winget, D. E. 2008, ApJ, 675, 1505
Bischoff-Kim, A., Østensen, R. H., Hermes, J. J., & Provencal, J. L. 2014, ApJ, 794, 39
Bradley, P. A. 1998, ApJS, 116, 307
Bradley, P. A. 2001, ApJ, 552, 326
Brickhill, A. J. 1991, MNRAS, 251, 673
Castanheira, B. G., & Kepler, S. O. 2008, MNRAS, 385, 430
Castanheira, B. G., & Kepler, S. O. 2009, MNRAS, 396, 1709
Castanheira, B. G., Kepler, S. O., Mullally, F., et al. 2006, A&A, 450, 227
Clemens, J. C., O'Brien, P. C., Dunlap, B. H., & Hermes, J. J. 2017, in Seismology of an Ensemble of ZZ Ceti Stars, eds. P.-E., Tremblay, B., Gänsicke, & T, March (San Francisco: ASP), ASP Conf. Ser., 509, 255
Córsico, A. H., & Althaus, L. G. 2006, A&A, 454, 863
Córsico, A. H., García-Berro, E., Althaus, L. G., & Isern, J. 2004, A&A, 427, 923
Córsico, A. H., Althaus, L. G., Montgomery, M. H., García-Berro, E., & Isern, J. 2005, A&A, 429, 277
Córsico, A. H., Althaus, L. G., & Miller Bertolami, M. M. 2006, A&A, 458, 259
Córsico, A. H., Romero, A. D., Althaus, L. G., & García-Berro, E. 2009, A&A, 506, 835
Córsico, A. H., Althaus, L. G., Miller Bertolami, M. M., et al. 2012, MNRAS, 424, 2792
Córsico, A. H., Romero, A. D., Althaus, L. G., et al. 2016, J. Cosmology Astropart. Phys., 7, 036
De Gerónimo, F. C., Althaus, L. G., Córsico, A. H., Romero, A. D., & Kepler, S. O. 2017, A&A, 599, A21
De Marco, O., & Soker, N. 2002, PASP, 114, 602
Dolez, N., & Vauclair, G. 1981, A&A, 102, 375
Fontaine, G., & Brassard, P. 2008, PASP, 120, 1043
Giammichele, N., Charpinet, S., Brassard, P., & Fontaine, G. 2017a, A&A, 598, A109
Giammichele, N., Charpinet, S., Fontaine, G., & Brassard, P. 2017b, ApJ, 834, 136
Gianninas, A., Bergeron, P., & Fontaine, G. 2006, AJ, 132, 831
Goldreich, P., & Wu, Y. 1999, ApJ, 511, 904
Greggio, L., & Renzini, A. 1990, ApJ, 364, 35
Han, Z., Tout, C. A., & Eggleton, P. P. 2000, MNRAS, 319, 215
Herwig, F., Bloecker, T., Schoenberner, D., & El Eid M. 1997, A&A, 324, L81
Isern, J., Hernanz, M., & García-Berro, E. 1992, ApJ, 392, L23
Isern, J., García-Berro, E., Althaus, L. G., & Córsico, A. H. 2010, A&A, 512, A86
Kanaan, A., Nitta, A., Winget, D. E., et al. 2005, A&A, 432, 219
Karakas, A. I., & Lattanzio, J. C. 2014, PASA, 31, e030
Kepler, S. O. & Romero, A. D. 2017, Eur. Phys. J. Web Conf., 152, 01011
Landolt, A. U. 1968, ApJ, 153, 151
Marino, A. F., Milone, A. P., Yong, D., et al. 2017, ApJ, submitted, [arXiv:1706.02278]
Metcalfe, T. S., Montgomery, M. H., & Kanaan, A. 2004, ApJ, 605, L133
Miller Bertolami, M. M. 2016, A&A, 588, A25
Miller Bertolami, M. M., Althaus, L. G., Unglaub, K., & Weiss, A. 2008, A&A, 491, 253
Montgomery, M. H., Klumpe, E. W., Winget, D. E., & Wood, M. A. 1999, ApJ, 525, 482
Montgomery, M. H., Metcalfe, T. S., & Winget, D. E. 2003, MNRAS, 344, 657
Mukadam, A. S., Mullally, F., Nather, R. E., et al. 2004, ApJ, 607, 982
Mukadam, A. S., Montgomery, M. H., Winget, D. E., Kepler, S. O., & Clemens, J. C. 2006, ApJ, 640, 956
Mullally, F., Thompson, S. E., Castanheira, B. G., et al. 2005, ApJ, 625, 966
Prada Moroni, P. G., & Straniero, O. 2002, ApJ, 581, 585
Pustynski, V.-V., & Pustylnik, I. 2006, in Stellar Evolution at Low Metallicity: Mass Loss, Explosions, Cosmology, eds. H. J. G. L. M. Lamers, N. Langer, T. Nugis, & K. Annuk ASP Conf. Ser., 353, 149
Renedo, I., Althaus, L. G., Miller Bertolami, M. M., et al. 2010, ApJ, 717, 183
Romero, A. D., Córsico, A. H., Althaus, L. G., et al. 2012, MNRAS, 420, 1462
Romero, A. D., Kepler, S. O., Córsico, A. H., Althaus, L. G., & Fraga, L. 2013, ApJ, 779, 58
Saio, H. 2013, Eur. Phys. J. Web Conf., 43, 05005
Salaris, M., Domínguez, I., García-Berro, E., et al. 1997, ApJ, 486, 413
Salaris, M., Althaus, L. G., & García-Berro, E. 2013, A&A, 555, A96
Segretain, L., Chabrier, G., Hernanz, M., et al. 1994, ApJ, 434, 641
Silvotti, R., Voss, B., Bruni, I., et al. 2005, A&A, 443, 195
Straniero, O., Domínguez, I., Imbriani, G., & Piersanti, L. 2003, ApJ, 583, 878
Tassoul, M., Fontaine, G., & Winget, D. E. 1990, ApJS, 72, 335
Tremblay, P.-E., Bergeron, P., & Gianninas, A. 2011, ApJ, 730, 128
Wachlin, F. C., Miller Bertolami, M. M., & Althaus, L. G. 2011, A&A, 533, A139
Winget, D. E., & Kepler, S. O. 2008, ARA&A, 46, 157
Winget, D. E., van Horn, H. M., Tassoul, M., et al. 1982, ApJ, 252, L65